Electronic Supplementary Information

Experimental Section

Materials: Carbon cloth was provided by Hongshan District, Wuhan Instrument Surgical Instruments Business. Sodium hypophosphite (NaH_2PO_2) was purchased from Aladdin Ltd. (Shanghai, China). $Na_2MoO_4 \cdot 2H_2O$, thiourea and H_2SO_4 were purchased from Beijing Chemical Corp. (China). KOH was purchased from Aladdin Ltd. (Shanghai, China). Pt/C (20 wt% Pt on Vulcan XC-72R) was purchased from Sigma-Aldrich. All chemicals were used as received without further purification. The water used throughout all experiments was purified through a Millipore system.

Preparation of MoS_2 NS/CC: In a typical synthesis, $Na_2MoO_4 \cdot 2H_2O$ (0.242 g) was dissolved in deionized water (22 mL) in a 50 mL beaker, into which thiourea (0.305 g) was added. After gentle stirring for 30 min, the solution was then transferred to a 40 mL Teflon-lined stainless steel autoclave with a piece of CC (2 cm × 3 cm) , the autoclave was sealed and heated at 220 °C for 24 h in an oven and then cooled down to room temperature naturally. Finally, the product was taken out, rinsed with deionized water several times and dried at 60 °C in air. The loading for MoS_2 nanosheet on CC was determined to be 4.3 mg cm^{-2} with a high precision microbalance.

Preparation of MoP_2 NS/CC: NaH_2PO_2 (1.0 g) was put at the center of front zone in a two-zone furnace, while MoS_2 NS/CC was put at the center of back zone. The temperature of the front zone was raised from 20–300 °C with a heating rate of 2 °C min^{-1} and held at this temperature for 60 min, meanwhile, the temperature of the

back zone was elevated from 20–700 °C with a heating rate of 5 °C min^{-1} and kept at this temperature for 64 min. After the conversion process, the furnace was allowed to cool down to room temperature under Ar. The loading for MoP_2 nanosheet on CC was calculated to be 7.8 mg cm^{-2} with a high precision microbalance.

Characterizations: SEM measurements were carried out on a XL30 ESEM FEG microscope at an accelerating voltage of 20 kV. Powder XRD data were acquired on a RigakuD/MAX 2550 diffractometer with $Cu_{K\alpha}$ radiation (λ = 1.5418 Å). XPS measurements were performed on an ESCALABMK II X-ray photoelectron spectrometer using Mg as the exciting source. BET surface area, pore volume and pore size were measured on a Quantachrome NOVA 1000 system at liquid N_2 temperature.

Electrochemical measurements: All the electrochemical measurements were conducted using a CHI660E potentiostat (CH Instruments, China) in a typical three-electrode setup, with a piece of freshly-made MoP_2 NS/CC or MoS_2 NS/CC as the working electrode, a graphite rod as the counter electrode and a saturated calomel electrode (SCE) as the reference electrode. Prior to every measurement, a resistance test was made and the *iR* compensation was applied to all initial data for further analysis. EIS measurements were carried out in the frequency range of 100 kHz–0.01 Hz. In all measurements, the SCE was calibrated with respect to RHE. In 0.5 M H_2SO_4, E (RHE) = E (SCE) + 0.281 V. In 1.0 M KOH, E (RHE) = E (SCE) + 1.068 V. In 1.0 M PBS, E (RHE) = E (SCE) + 0.655 V. LSV curves were conducted in electrolyte with a scan rate of 5 mV s^{-1}. All the potentials reported in our work were

expressed *vs*. the RHE.

TOF calculation: The number of active sites was quantified by CV scanning from -0.2–0.6 V *vs*. RHE in phosphate buffer (pH = 7) at a scan rate of 50 mV/s, which is proportional to the integrated charge in this potential range without obvious redox peaks. Concretely, n = Q/2F, where n is the number of active sites; Q is the voltammetric charge and F is the Faraday constant (96485.3 C mol^{-1}). Considering the fact of TOF = *I*/2nF (*I* is the current during the LSV measurement in acid), the formula of TOF = *I*/Q could be easily derived.

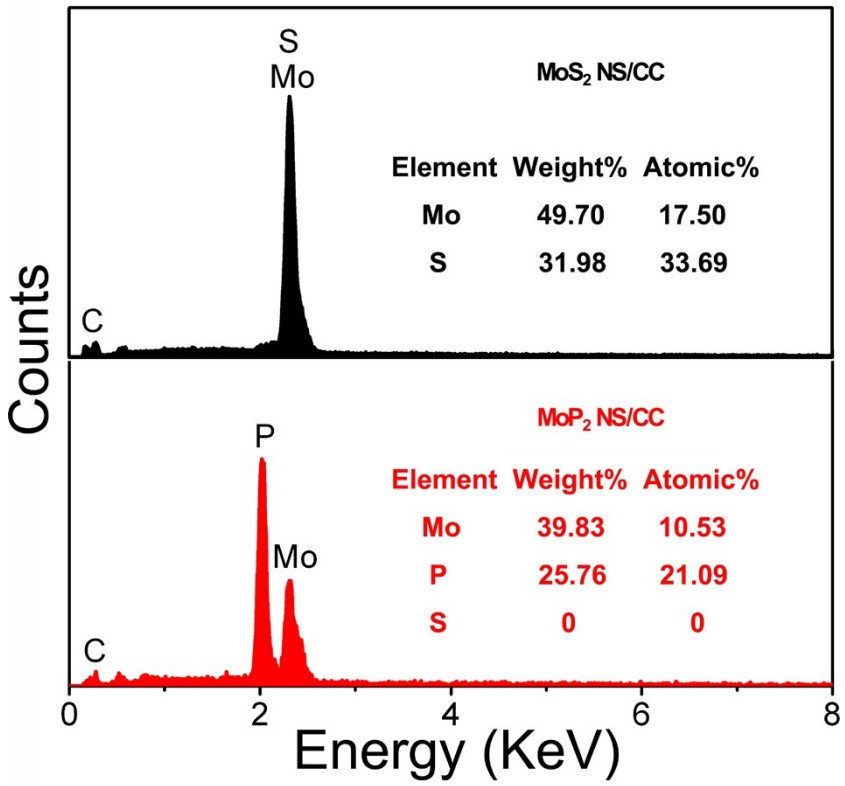

Fig. S1. EDX spectra of MoS_2 NS/CC and MoP_2 NS/CC.

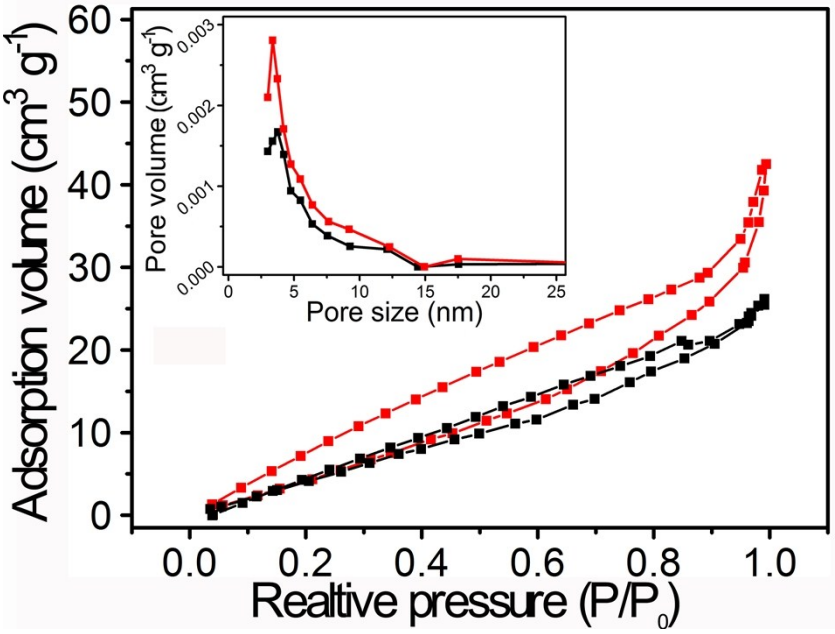

Fig. S2. Nitrogen adsorption/desorption isotherms and the BJH pore-size distribution curves (inset) of MoP_2 (red curve) and MoS_2 (black curve).

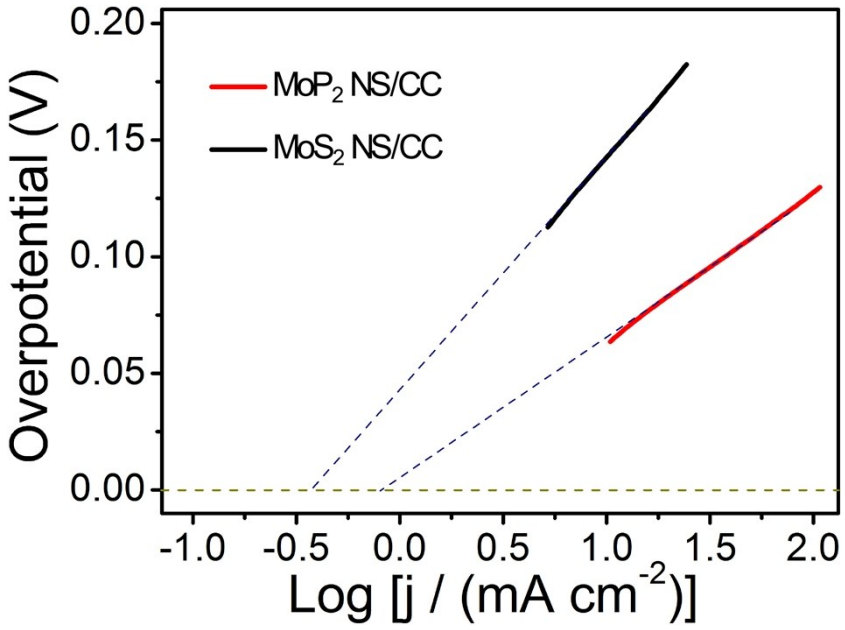

Fig. S3. Tafel plots used for calculating exchange current densities of MoP_2 NS/CC and MoS_2 NS/CC by extrapolation method.

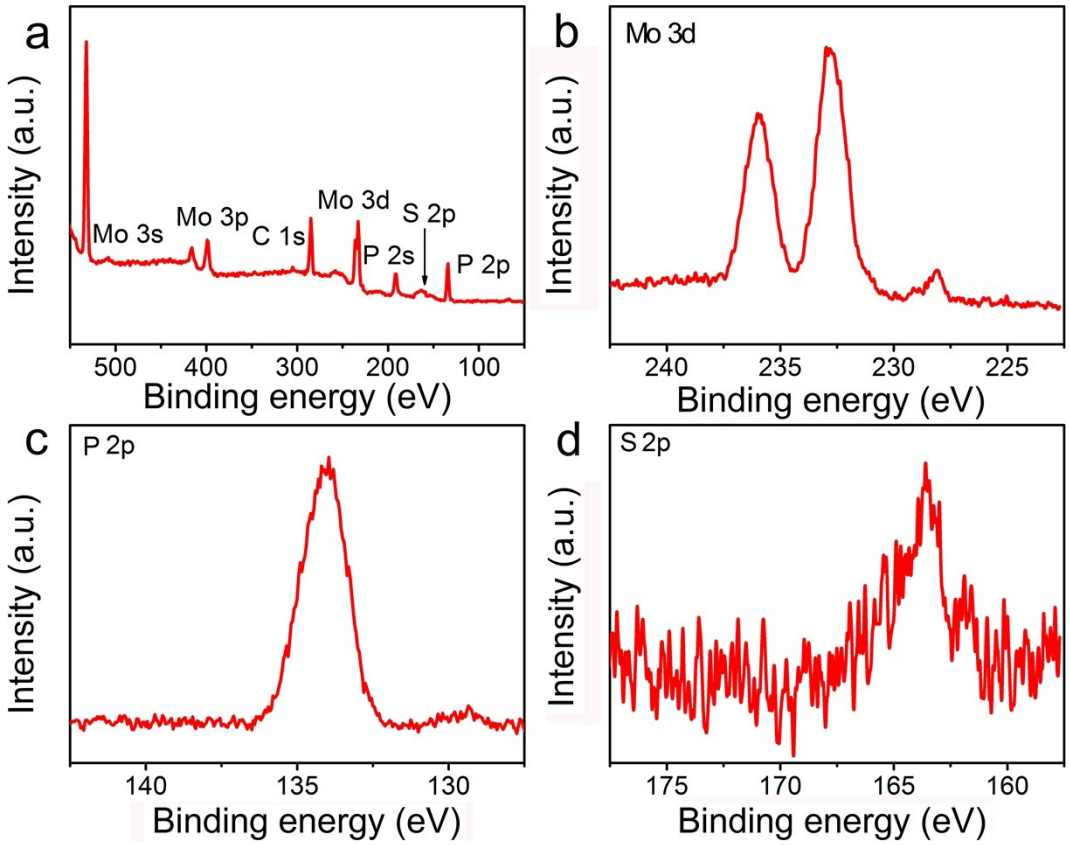

Fig. S4. a) Survey XPS spectra of the partially converted product. XPS spectra in b) Mo 3d, c) P 2p and d) S 2p regions.

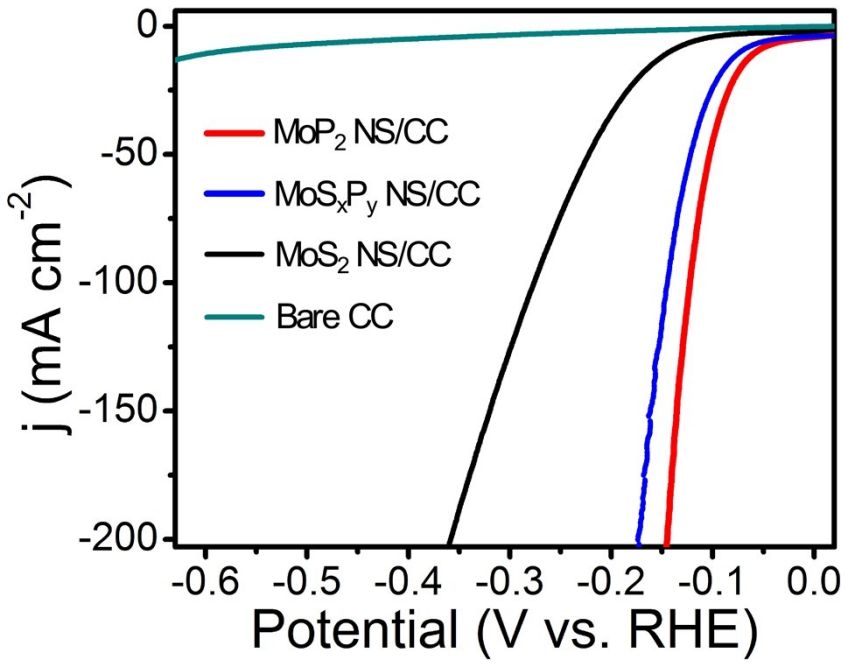

Fig. S5. Comparison of HER performances of MoP_2 NS/CC, MoS_xP_y NS/CC, MoS_2 NS/CC and bare CC in 0.5 M H_2SO_4.

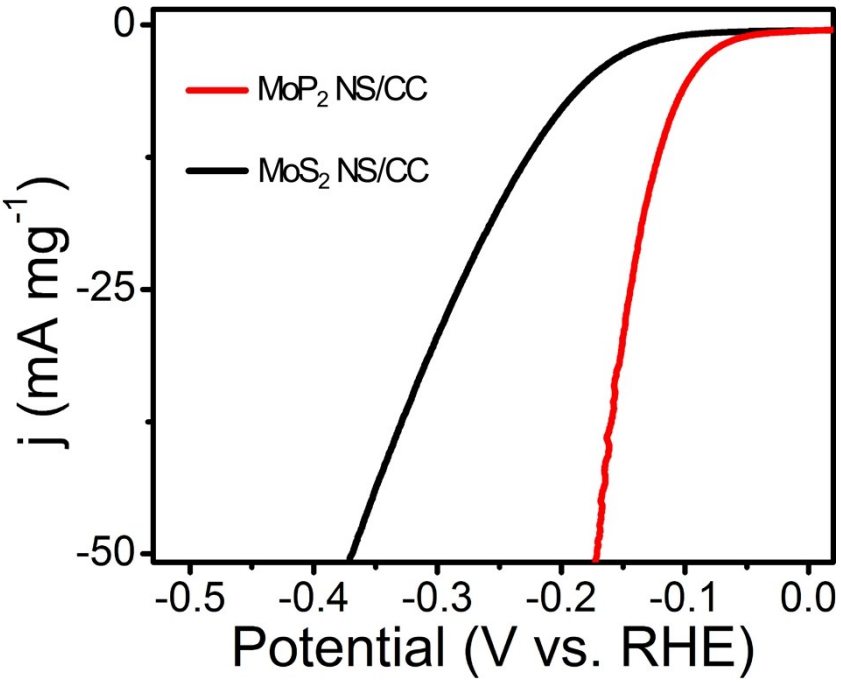

Fig. S6. Mass-normalized polarization curves of MoP_2 NS/CC and MoS_2 NS/CC in 0.5 M H_2SO_4 with a scan rate of 5 mV/s.

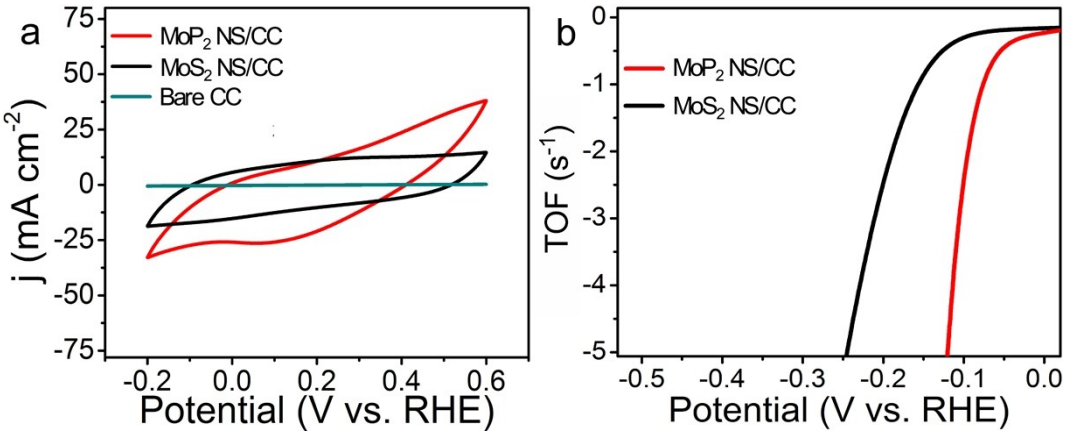

Fig. S7. a) CVs of MoP_2 NS/CC, MoS_2 NS/CC and bare CC in 1.0 M PBS (pH = 7) with a scan rate of 50 mV s^{-1}. b) Calculated TOFs for MoP_2 NS/CC and MoS_2 NS/CC in 0.5 M H_2SO_4.

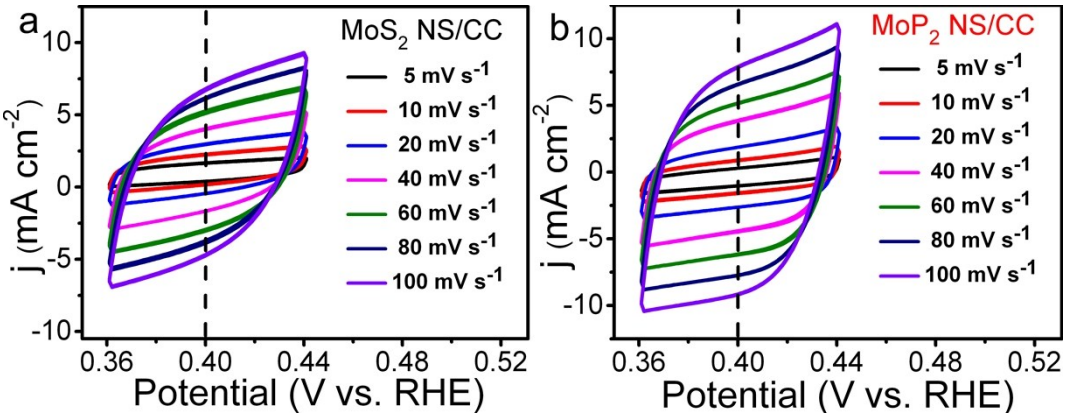

Fig. S8. Typical cyclic voltammograms of a) MoS_2 NS/CC and b) MoP_2 NS/CC with various scan rates (5–100 mV s^{-1}) in the region of 0.36–0.44 V (*vs.* RHE) in 0.5 M H_2SO_4.

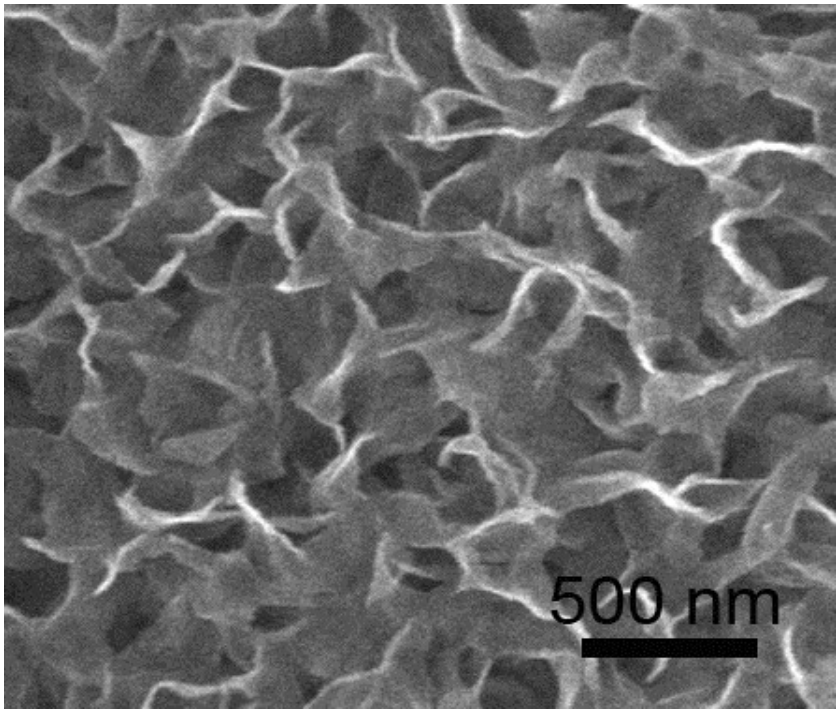

Fig. S9. SEM image of MoP_2 NS/CC after 2000 successive CV cycles in 0.5 M H_2SO_4.

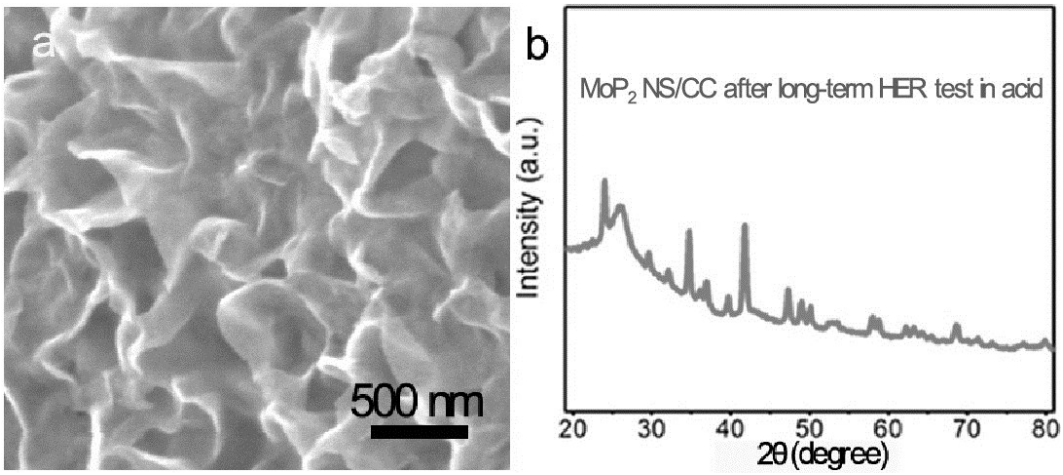

Fig. S10. a) SEM image and b) XRD pattern of MoP_2 NS/CC after long-term HER test in 0.5 M H_2SO_4.

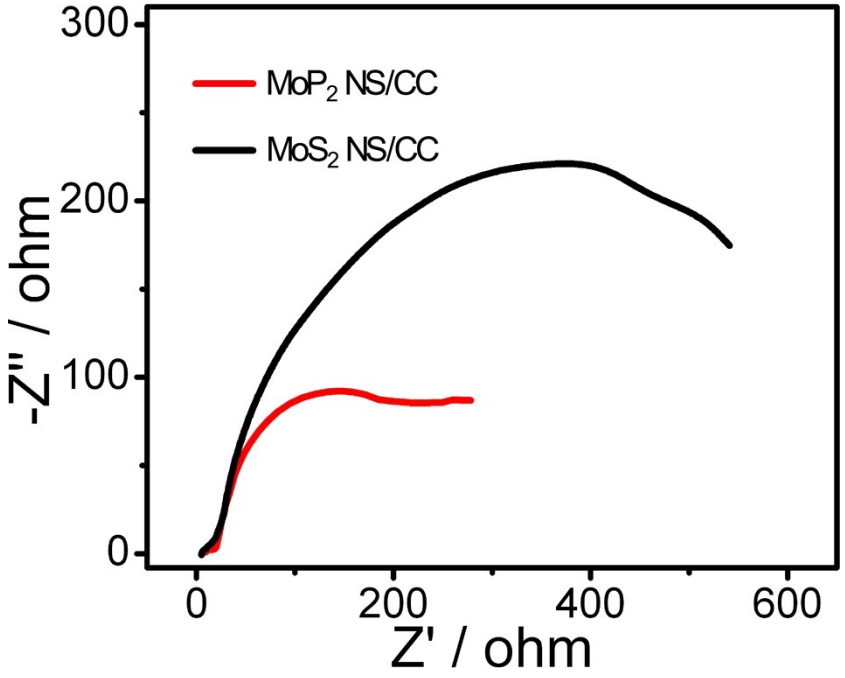

Fig. S11. Nyquist plots of MoP_2 NS/CC and MoS_2 NS/CC in 1.0 M KOH at open circuit potential.

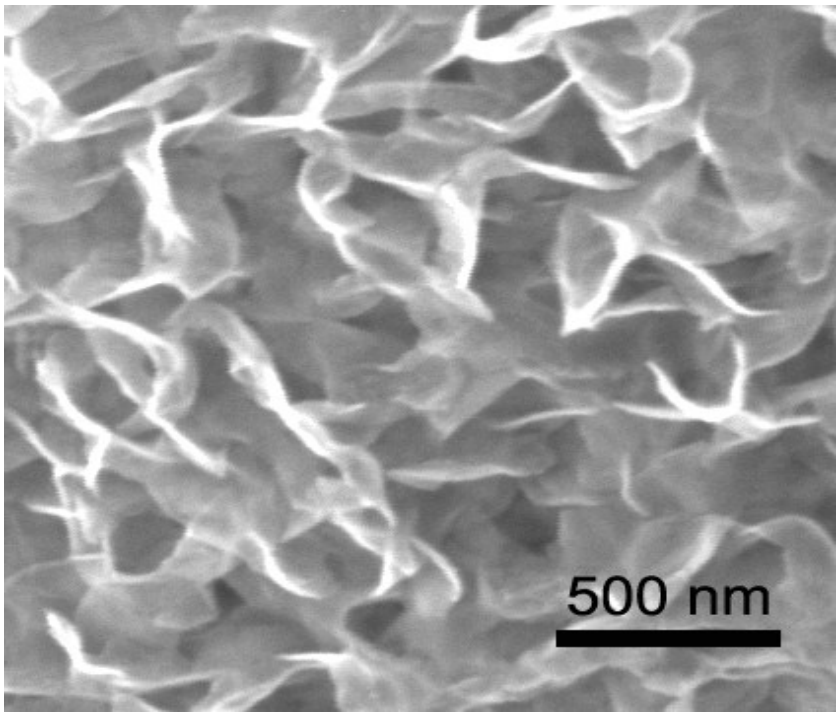

Fig. S12. SEM image of MoP_2 NS/CC after 2000 successive CV cycles in 1.0 M KOH.

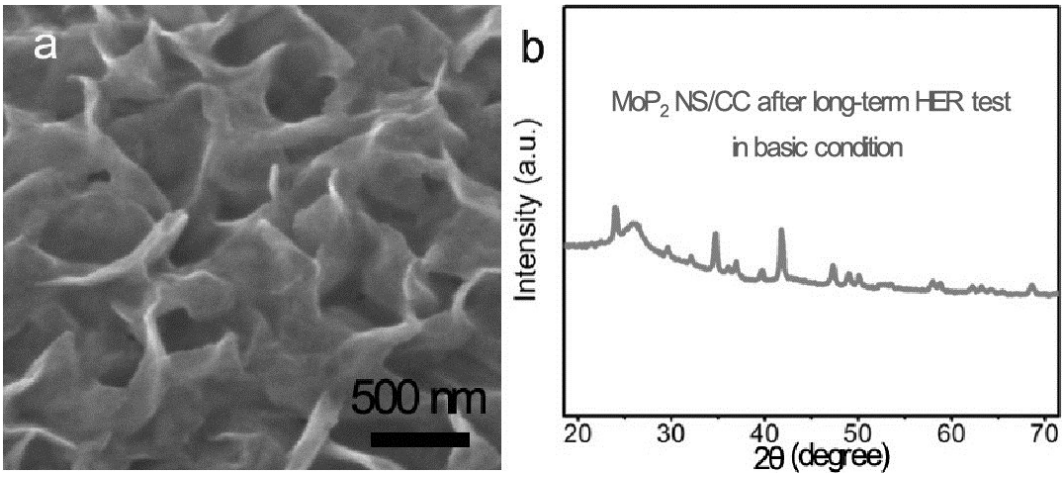

Fig. S13. a) SEM image and b) XRD pattern of MoP_2 NS/CC after long-term HER test in basic condition.

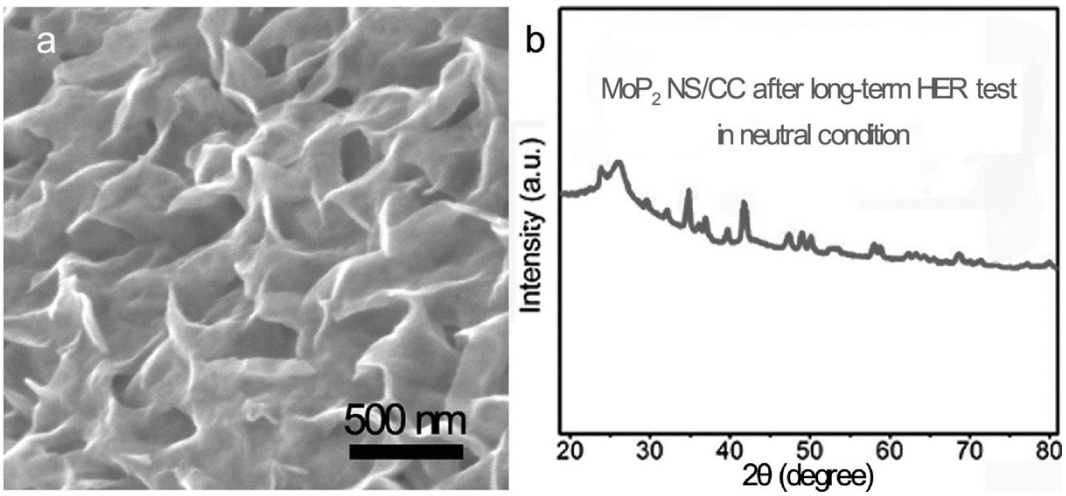

Fig. S14. a) SEM image and b) XRD pattern of MoP_2 NS/CC after long-term HER test in neutral condition.

Table S1 Comparison of HER performance in 0.5 M H_2SO_4 for MoP_2 NS/CC with other Mo-based HER catalysts ([a] catalysts directly grown on current collectors).

Catalyst	Current density (j, mA cm^{-2})	Overpotential at the corresponding j (mV)	Ref.
metallic MoS_2 nanosheet	10	195	1
defect-rich MoS_2	13	200	2
interconnected MoP nanoparticle	10	125	3
MoP nanosheet/carbon flake	10.1	200	4
$MoS_{2(1-x)}Se_{2x}$	10	164	5
nanoporous Mo_2C nanowire	60	200	6
β-Mo_2C	10	172	7
Mo_2C@CNTs	10	152	8
3D MoP sponge[a]	10	105	9
MoP|S	10	64	10
$MoS_{2(1-x)}P_x$	10	150	11
amorphous MoP nanoparticle	10	90	12
MoP_2 NS/CC[a]	10	58	This work

Table S2 Comparison of HER performance in 1.0 M KOH for MoP_2 NS/CC with other non-noble metal HER catalysts ([a] catalysts directly grown on current collectors).

Catalyst	Current density (j, mA cm^{-2})	Overpotential at the corresponding j (mV)	Ref.
β-Mo_2C	10	112	7
CoP/CC[a]	10	209	13
NiP_2/CC[a]	10	102	14
FeP/Fe foil[a]	10	194	15
FeP_2/Fe foil[a]	10	189	15
Ni-Mo/Ti mesh[a]	10	92	16
NiSe/Ni foam[a]	10	96	17
Ni-P/Cu foam[a]	10	98	18
Ni-P/Ni foam[a]	10	80	19
NiO/Ni-CNT	10	< 100	20
NiS/Ni foam[a]	10	~ 120	21
MoP_2 NS/CC[a]	10	67	This work

Table S3 Comparison of HER performance in 1.0 M PBS (pH = 7) for MoP_2 NS/CC with other non-noble metal HER catalysts ([a] catalysts directly grown on current collectors).

Catalyst	Current density (j, mA cm^{-2})	Overpotential at the corresponding j (mV)	Ref.
CoP/CC[a]	10	106	13
Ni-B/Cu plate[a]	10	54	22
Co-B nanoparticles	10	251	23
NiS_2/CC[a]	10	243	24
WP/CC[a]	10	200	25
Co_9S_8/CC[a]	10	175	26
MoS_2/Ti plate[a]	10	200	27
Ni_3S_2/Ni foam[a]	10	170	28
MoP_2 NS/CC[a]	10	85	This work

References

1 M. A. Lukowski, A. S. Daniel, F. Meng, A. Forticaux, L. Li and S. Jin, *J. Am. Chem. Soc.*, 2013, **135**, 10274.

2 J. Xie, H. Zhang, S. Li, R. Wang, X. Sun, M. Zhou, J. Zhou, X. Lou and Y. Xie, *Adv. Mater.*, 2013, **25**, 5807.

3 Z. Xing, Q. Liu, A. M. Asiri and X. Sun, *Adv. Mater.*, 2014, **26**, 5702.

4 W. Cui, Q. Liu, Z. Xing, A. M. Asiri, K. A. Alamry and X. Sun, *Appl. Catal. B: Environ.*, 2015, **164**, 144.

5 Q. Gong, L. Cheng, C. Liu, M. Zhang, Q. Feng, H. Ye, M. Zeng, L. Xie, Z. Liu and Y. Li, *ACS Catal.*, 2015, **5**, 2213.

6 L. Liao, S. Wang, J. Xiao, X. Bian, Y. Zhang, M. Scanlon, X. Hu, Y. Tang, B. Liu and H. H. Girault, *Energy Environ. Sci.*, 2014, **7**, 387.

7 F. Ma, H. Wu, B. Xia, C. Xu and X. Lou, *Angew. Chem. Int. Ed.*, 2015, **54**, 15395.

8 W. Chen, C. Wang, K. Sasaki, N. Marinkovic, W. Xu, J. T. Muckerman, Y. Zhu and R. R. Adzic, *Energy Environ. Sci.*, 2013, **6**, 943.

9 C. Deng, F. Ding, X. Li, Y. Guo, W. Ni, H. Yan, K. Sun and Y. Yan, *J. Mater. Chem. A*, 2016, **4**, 59.

10 J. Kibsgaard and T. F. Jaramillo, *Angew. Chem. Int. Ed.*, 2014, **53**, 14433.

11 R. Ye, P. Angel-Vicente, Y. Liu, M. J. Arellano-Jimenez, Z. Peng, T. Wang, Y. Li, B. I. Yakobson, S.-H. Wei, M. J. Yacaman and J. M. Tour, *Adv. Mater.*, 2016, **28**, 1427.

12 J. M. McEnaney, J. C. Crompton, J. F. Callejas, E. J. Popczun, A. J. Biacchi, N. S. Lewis and R. E. Schaak, *Chem. Mater.*, 2014, **26**, 4826.

13 J. Tian, Q. Liu, A. M. Asiri and X. Sun, *J. Am. Chem. Soc.*, 2014, **136**, 7587.

14 P. Jiang, Q. Liu and X. Sun, *Nanoscale*, 2014, **6**, 13440.

15 C. Y. Son, I. H. Kwak, Y. R. Lim and J. Park, *Chem. Commun.*, 2016, **52**, 2819.

16 J. Tian, N. Cheng, Q. Liu, X. Sun, Y. He and A. M. Asiri, *J. Mater. Chem. A*, 2015, **3**, 20056.

17 C. Tang, N. Cheng, Z. Pu, W. Xing and X. Sun, *Angew. Chem. Int. Ed.*, 2015, **54**,

9351.

18 Q. Liu, S. Gu and C. M. Li, *J. Power Sources*, 2015, **299**, 342.

19 C. Tang, A. M. Asiri, Y. Luo and X. Sun, *ChemNanoMat*, 2015, **1**, 558.

20 M. Gong, W. Zhou, M.-C. Tsai, J. Zhou, M. Guan, M. Lin, B. Zhang, Y. Hu, D. Wang, J. Yang, S. J. Pennycook, B.-J. Hwang and H. Dai, *Nat. Commun.*, 2014, **5**, 4695.

21 W. Zhu, X. Yue, W. Zhang, S. Yu, Y. Zhang, J. Wang and J. Wang, *Chem. Commun.*, 2016, **52**, 1486.

22 P. Zhang, M. Wang, Y. Yang, T. Yao, H. Han and L. Sun, *Nano Energy*, 2016, **19**, 98.

23 S. Gupta, N. Patel, A. Miotello and D. Kothari, *J. Power Sources*, 2015, **279**, 620.

24 C. Tang, Z. Pu, Q. Liu, A. M. Asiri and X. Sun, *Electrochim. Acta*, 2015, **153**, 508.

25 Z. Pu, Q. Liu, A. M. Asiri and X. Sun, *ACS Appl. Mater. Interfaces*, 2014, **6**, 21874.

26 L.-L. Feng, M. Fan, Y. Wu, Y. Liu, G.-D. Li, H. Chen, W. Chen, D. Wang and X. Zou, *J. Mater. Chem. A*, 2016, DOI: 10.1039/C5TA08611F.

27 J. Shi and J. Hu, *Electrochim. Acta*, 2015, **168**, 256.

28 L.-L. Feng, G. Yu, Y. Wu, G.-D. Li, H. Li, Y. Sun, T. Asefa, W. Chen and X. Zou, *J. Am. Chem. Soc.*, 2015, **137**, 14023.